01 Jan 1980

MTI Improvement Factors For Weighted DFTs

Rodger E. Ziemer
Missouri University of Science and Technology

Recommended Citation

R. E. Ziemer, "MTI Improvement Factors For Weighted DFTs," *IEEE Transactions on Aerospace and Electronic Systems*, vol. AES thru 16, no. 3, pp. 393 - 397, Institute of Electrical and Electronics Engineers, Jan 1980.
The definitive version is available at https://doi.org/10.1109/TAES.1980.308908

Correspondence

MTI Improvement Factors for Weighted DFTs

Abstract

The use of the discrete Fourier transform (DFT) to enhance the detection of moving targets in ground clutter is examined. The improvement factor, defined as the signal-to-clutter ratio at the DFT processor output compared with that of the input, is given as a function of normalized clutter spectral width for various weighting functions on the DFT input. The effect of quantization of the weights on the improvement factor is also examined.

I. Introduction

The use of the discrete Fourier transform (DFT) to determine the velocity of moving targets by means of coherent pulse-Doppler radar systems has become common with the availability of high-speed digital processors. In pulse-Doppler radar-system implementations, a clutter canceller often precedes the Doppler filter bank in order to improve the detectability of the target in the presence of ground clutter entering the radar receiver through the mainlobe of the antenna pattern (so-called main beam clutter).

The signal-to-clutter ratio enhancement provided by multiple delay-line cancellers has been analyzed for various configurations and appears in the literature [1]. An alternative scheme for mainlobe clutter rejection in DFT-processing radar receivers is to simply not use the DFT outputs in the vicinity of the main beam clutter spectrum, which is typically tracked and centered at zero frequency. For processors where sample values are represented by binary numbers with a small number of bits (say eight or less), both techniques may be employed due to the limited dynamic range of the processor. Recently, however, digital hardware has become available which makes possible the implementation of processors employing 12- or 16-bit number representations. In such cases it is feasible to employ the DFT clutter rejection scheme alone. In addition to being simpler, the elimination of the clutter canceller results in uncorrelated noise samples at the DFT input, which in turn results in higher overall processing gain [2].

It is the purpose of this correspondence to examine the influence of various types of DFT weighting functions on the clutter improvement factor, as well as the impact of the number of bits used in representing the weights.

II. Derivation of Improvement Factor

It is convenient and reasonable to assume a Gaussian spectrum of the form

Manuscript received September 17, 1979; revised December 26, 1979.

0018-9251/80/0500-0393 $00.75 ©1980 IEEE

$$C(f) = M_0 \exp(-K^2 f^2) \tag{1}$$

for the main beam clutter. For airborne platforms, the constant K can be related to the azimuthal beamwidth of the antenna pattern Θ_B, the wavelength of the radiated waveform λ, the radar platform velocity V, the antenna azimuth angle Θ_0, and depression angle ϕ_0, as

$$K = \sqrt{k}\ \lambda \csc \Theta_0 \sec \phi_0 / (2V\Theta_B) \tag{2}$$

where $k = 5.5452$ to place the one-way −3-dB power response of the antenna at $\Theta = \Theta_B/2$. This expression ignores the effects of phenomena such as scanning and shear wind which are secondary for airborne applications.

The autocorrelation function corresponding to the clutter spectrum given by (1) results from application of the Fourier transform pair [3]

$$\exp[-\pi(t/\tau_0)^2] \leftrightarrow \tau_0 \exp[-\pi(\tau_0 f)^2]\ . \tag{3}$$

It is

$$R_c(\tau) = M_0 \tau_0^{-1} \exp[-(\pi\tau/K)^2] \tag{4}$$

where

$$\tau_0 = (K^2/\pi)^{1/2}\ . \tag{5}$$

Now the output of the DFT at its kth frequency (hereafter referred to as DFT filter number k) is given by

$$X(k) = \sum_{n=0}^{N-1} w(n)\, x(n) \exp(-2j\pi kn/N) \tag{6}$$

where N is the number of DFT points and $w(0), w(1), \ldots, w(N-1)$ are a set of input weights. The input samples to the DFT consist of signal plus clutter, and may be expressed as

$$x(n) = x_s(n) + x_c(n) \tag{7}$$

where the subscript s denotes signal and the subscript c denotes clutter. Thus the DFT output in filter k can be represented as

$$X(k) = X_s(k) + X_c(k) \tag{8}$$

where expressions for $X_s(k)$ and $X_c(k)$ can be obtained from (6) by replacing $x(n)$ by $x_s(n)$ and $x_c(n)$ respectively.

Assuming a coherently pulsed sinusoidal input signal to the receiver, it follows that the input to the DFT, which includes both in-phase and quadrature low-pass signal components, can be represented as

$$x_s(n) = A_s \exp[j(2\pi\beta n/N + \theta)] \tag{9}$$

where β is the normalized frequency (fT_p, where T_p equals the sampling time) of $x_s(t)$ and θ is a random phase angle. It follows that the power in the signal component at the kth filter output of the DFT is

$$\overline{|X_s(k)|^2} = A_s^2 \sum_{n,m=0}^{N-1}\sum w(n)w(m) \exp[j2\pi(\beta - k)(n-m)/N]\ . \tag{10}$$

The clutter power at the output of the kth filter, found by taking the ensemble average of the product of

$$X_c(k) = \sum_{n=0}^{N-1} w(n)x_c(n) \exp[-j2\pi kn/N] \tag{11}$$

with its complex conjugate, is [2]

$$\overline{|X_c(k)|^2} = 2 \sum_{n,m=0}^{N-1}\sum \hat{R}_c(n-m)w(n)w(m) \cos[2\pi k(n-m)/N] \tag{12}$$

where, from (4), the sampled autocorrelation function of one quadrature component is given by

$$\hat{R}_c(n-m) = R_c[(n-m)T_p] = M_0\tau_0^{-1} \exp\{-[\pi(n-m)T_p/K]^2\}\ . \tag{13}$$

The interpulse period (IPP), T_p, has been introduced in (13) as a result of the sampling by the digital processor at IPP intervals.

The signal-to-clutter power ratio at the kth DFT output filter is the ratio of (10) to (12). The moving target indicator (MTI) improvement factor F is defined as the signal-to-clutter power ratio at the output of the kth DFT filter divided by the signal-to-clutter power ratio at the receiver input for a signal with normalized frequency $\beta = k$. It is

$$F = \left[\sum_{n=0}^{N-1} w(n)\right]^2 \Big/ \sum_{n,m=0}^{N-1}\sum w(n)w(m) \cdot \exp\{-[\sqrt{2}\,\pi(n-m)\sigma_n]^2\} \cos[2\pi k(n-m)/N] \tag{14}$$

where σ_n is the clutter spectral spread (standard deviation) normalized by the pulse repetition frequency f_p and can be expressed in terms of T_p as

$$\sigma_n = T_p/\sqrt{2}K\ . \tag{15}$$

III. Results

Equation (14) was evaluated by computer for various sets of weighting coefficients for both unquantized and quantized weights. The weighting sets employed are summarized in Table I along with their equivalent noise bandwidths [4]. The MTI improvement factor is plotted versus the normalized spectral spread in Figs. 1-3 for the Hanning, Hamming, and Blackman weighting functions. Figs. 4-10 shown similar plots for the Kaiser-Bessel weight-

0018-9251/80/0500-0394 $00.75 ©1980 IEEE

TABLE I

Weighting Functions and Corresponding Equivalent Noise Bandwidths

Weight function name	Mathematical specification of $w(n)$ $n = 0, 1, ..., N-1$	Equivalent noise bandwidth normalized to frequency resolution
Hanning	$0.5[1 - \cos(2n\pi/N)]$	1.500
Hamming	$0.54 - 0.46\cos(2n\pi/N)$	1.363
Blackman	$0.42 - 0.5\cos(2n\pi/N) + 0.08\,(4n\pi/N)$	1.727
Kaiser-Bessel	$\dfrac{I_0\,[\pi\alpha\sqrt{1-(2n/N-1)^2}\,]}{I_0\,[\pi\ \alpha]}$	1.393 ($\alpha = 1.5$) 1.509 ($\alpha = 2.0$) 1.654 ($\alpha = 2.5$) 1.796 ($\alpha = 3.0$) 2.053 ($\alpha = 4.0$)

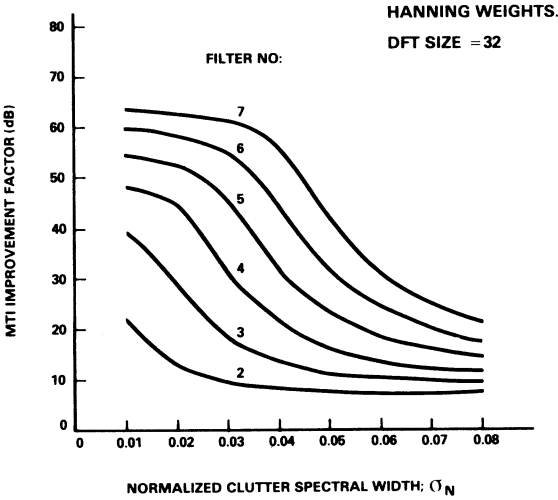

Fig. 1. MTI improvement factor for Hanning weights.

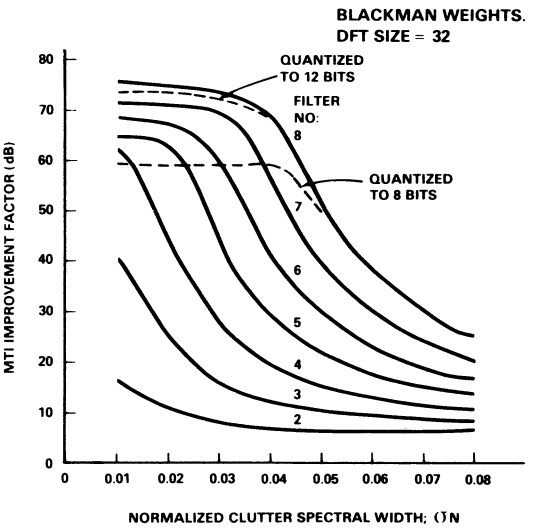

Fig. 3. MTI improvement factor for Blackman weights.

Fig. 2. MTI improvement factor for Hamming weights.

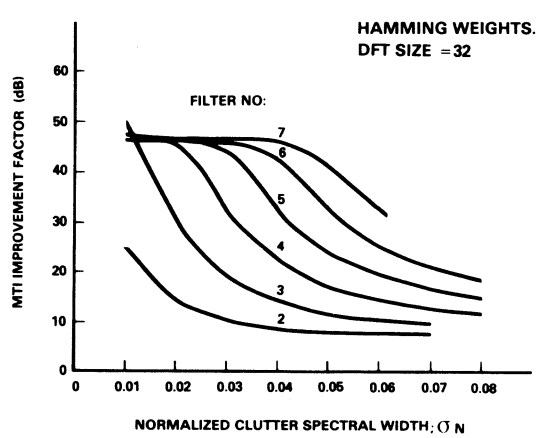

Fig. 4. MTI improvement factor for Kaiser-Bessel weights; $\alpha = 1.5$.

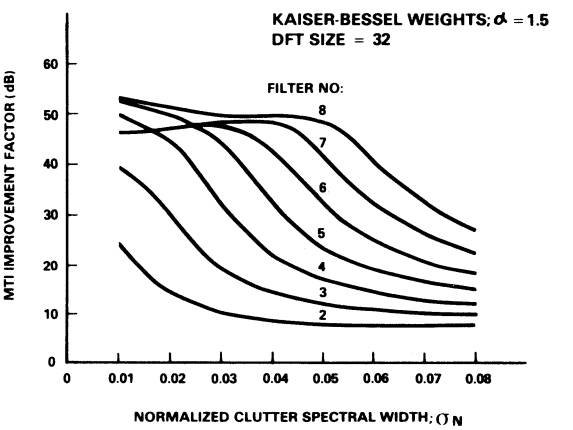

0018-9251/80/0500-0395 $00.75 ©1980 IEEE

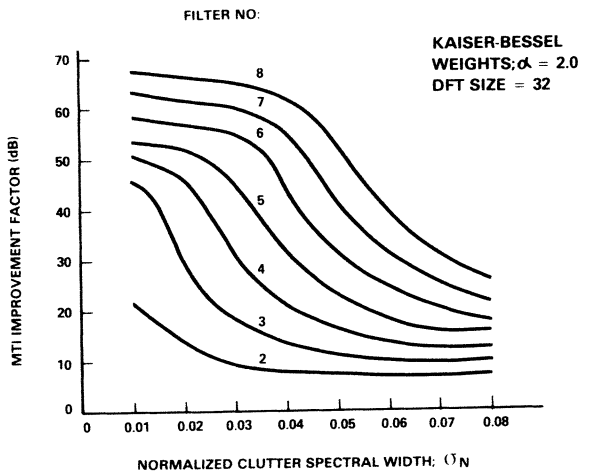

Fig. 5. MTI improvement factor for Kaiser-Bessel weights; $\alpha = 2.0$.

Fig. 6. MTI improvement factor for Kaiser-Bessel weights; $\alpha = 2.5$.

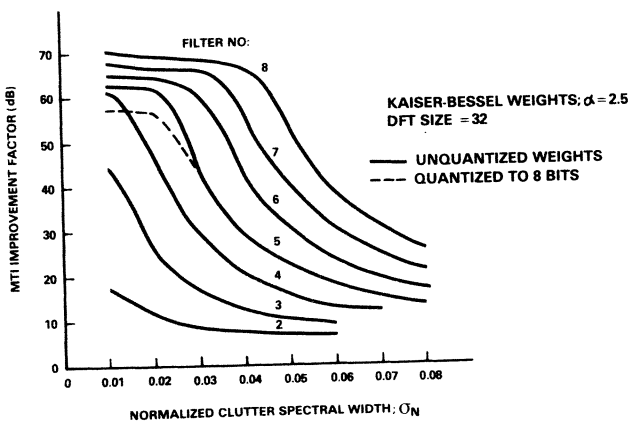

Fig. 7. MTI improvement factor for Kaiser-Bessel weights; $\alpha = 3.0$.

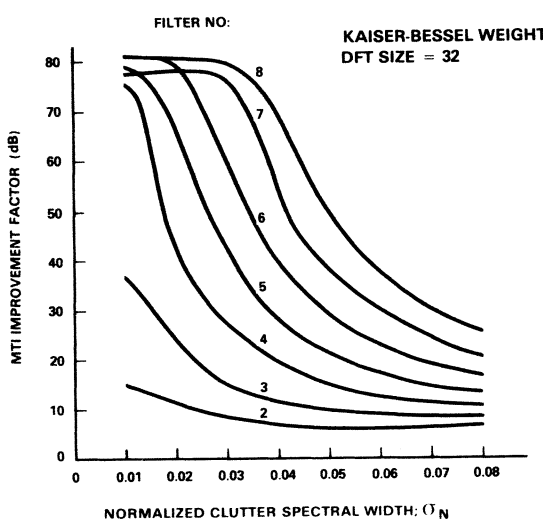

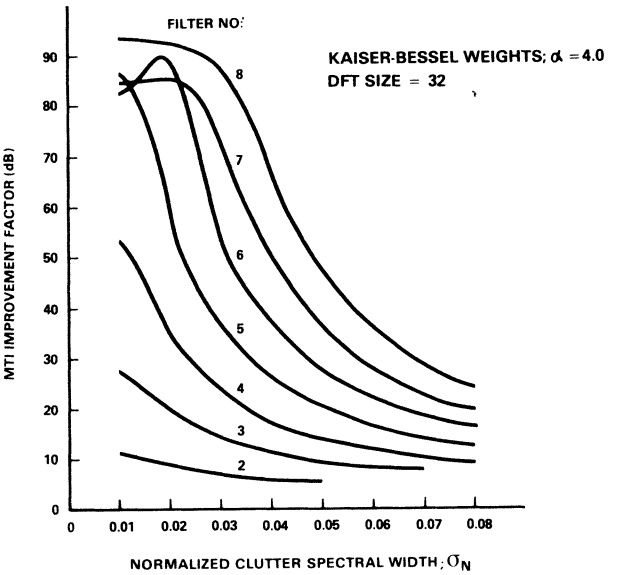

Fig. 8. MTI improvement factor for Kaiser-Bessel weights; $\alpha = 4.0$.

Fig. 9. MTI improvement factor for a 16-point, Kaiser-Bessel weighted DFT with $\alpha = 2.5$.

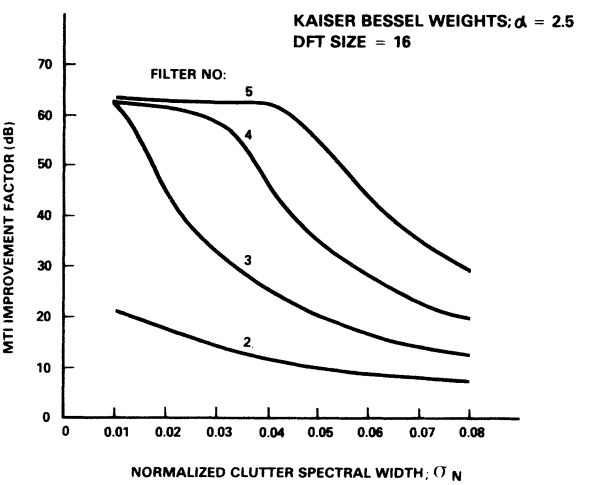

Fig. 10. MTI improvement factor for a 64-point Kaiser-Bessel weighted DFT with $\alpha = 2.5$.

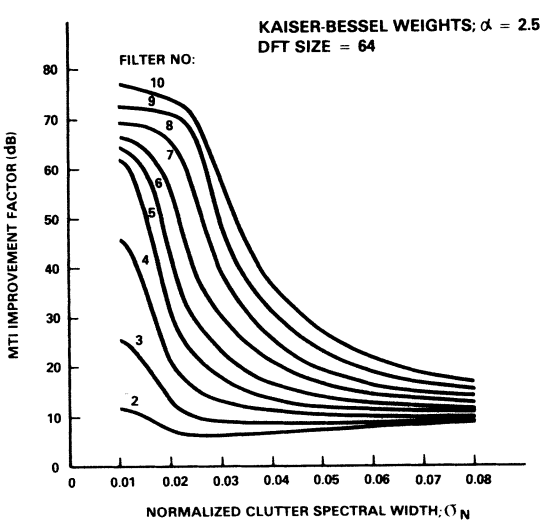

0018-9251/80/0500-0396 $00.75 ©1980 IEEE

ing function for various values of the window parameter α and for various DFT sizes. These figures illustrate how the improvement factor can be bounded by selectively discarding DFT filter outputs. In the improvement factor computations, the clutter is centered in the zeroth filter. The labeled curves show the improvement factor for both the filter listed and the corresponding image filter. Hence, all lower filters and corresponding image filters are discarded to achieve the desired improvement factor. Filter 1 is not shown because it sufficiently overlaps the clutter region as to provide a negligible improvement factor. Likewise, curves are not plotted for filter numbers higher than 8 for the 32-point DFT because this already entails greater than 50 percent bandstop filtering.

It is interesting to compare Figs. 1-3. For example, suppose $F \geqslant 60$ dB is required for $0 \leqslant \sigma_n \leqslant 0.03$. For Hanning weights, DFT filter number 7 provides at least 60-dB improvement for σ_n in this range, while filter number 6 suffices if Blackman weights are employed. Hamming weights were designed to provide constant sidelobes with -44 dB peaks [4]; hence, the improvement factor is bounded by this constraint.

The Kaiser-Bessel weighting function is convenient because of the possibility of trading mainlobe width for sidelobe level of its frequency spectrum by varying the parameter α. For example, Figs. 4-10 show that filter number 5 of a 32-point DFT provides at least 50 dB of MTI improvement for the following ranges of σ_n and corresponding values of α: $\sigma_n \leqslant 0.02$ if $\alpha = 1.5$; $\sigma_n \leqslant 0.024$ if $\alpha = 2.0$; $\sigma_n \leqslant 0.028$ if $\alpha = 2.5$; $\sigma_n \leqslant 0.026$ if $\alpha = 3.0$; and $\sigma_n \leqslant 0.023$ if $\alpha = 4.0$. Thus increasing α does not necessarily provide a larger clutter spectral width over which a minimum MTI improvement factor is attained. Increasing α does appear to provide a larger *maximum* MTI improvement factor, however, as can be seen by comparing curves for the same filter number for a fixed value of σ_n, say $\sigma_n = 0.02$.

The effects of quantized weights on the improvement factor are shown in Figs. 3 and 6 by the dashed curves. The quantization specifications *include sign*; thus 8 bits of quantization means 7 bits of magnitude plus a sign bit, even though the weights are all positive. Quantization of the weights results in the occurrence of spurious sidelobes in the magnitude spectrum of the weighting function. Quantization of input samples and subsequent roundoff or truncation errors in the DFT, which are not included in this analysis, can be characterized as an additive noise source as long as nonlinear effects such as saturation and deadbanding are negligible. Note from Fig. 3 that improvement factors in excess of 70 dB can be achieved with 12-bit arithmetic, and that 8-bit arithmetic provides a maximum improvement of not quite 60 dB. Some results for 16-bit weight representation were run and found to provide virtually identical results to the unquantized cases for the range of parameters considered. The effect of DFT length on MTI improvement factor can be studied with the aid of Figs. 9, 6, and 10, for which Kaiser-Bessel weights having $\alpha = 2.5$ were employed for DFT lengths of 16, 32, and 64, respectively. In comparing these figures, one should keep in mind that the DFT resolution increases by a factor of two with the doubling of the DFT size. Thus, for example, one should compare MTI improvement factors for filter number 2 in Fig. 9 with those of filter number 4 in Fig. 6, and with those of filter number 8 in Fig. 10. The advantage of a larger DFT size is apparent when one considers the superior improvement characteristics for filter number 8 of a 64-point DFT with the very poor characteristics of filter number 2 of a 16-point DFT.

As an example of using these curves for system design, consider an airborne radar for which the wavelength is 0.1 ft, the azimuthal beamwidth is 4.4°, and the pulse repetition frequency is 10 kHz. Suppose, further, that the platform velocity is 1500 ft/s and that the antenna scans a ± 45° sector in azimuth. From equations (15) and (2), the maximum value of σ_n occurs for $\Theta_0 = 45°$, and its value is 0.04891. A 32-point DFT length is desired. If a 40-dB minimum MTI improvement factor is desired, one would need to discard filters 1-6 for Hanning Hamming, and Blackman weights. For Kaiser-Bessel weights, filters 1-6 would be discarded for $\alpha = 1.5$, $\alpha = 2.0$, and $\alpha = 2.5$, filters 1-7 for $\alpha = 3.0$, and filters 1-7 for $\alpha = 4.0$. Note that although only filters 1-6 need to be discarded for $\alpha = 1.5$, the maximum improvement factor for any value of σ_n is limited to about 52 dB. To achieve a larger minimum improvement factor, one must use a larger value of α.

Acknowledgment

We wish to express our appreciation to Mr. Terry Lewis of Environmental Research Institute of Michigan, who initiated this study effort while an employee of Emerson Electric Company.

R.E. ZIEMER

Electrical Engineering Department
University of Missouri, Rolla
Rolla, MO 65401

J.A. ZIEGLER

Emerson Electric Company
Electronics and Space Division
St. Louis, MO 63136

References

[1] F. Nathanson, *Radar Design Principles.* New York: McGraw-Hill, 1969, p. 331ff.

[2] R.E. Ziemer, T. Lewis, and L. Guthrie, "Degradation analysis in pulse Doppler radars due to digital processing," *Proc. IEEE 1977 National Aerospace and Electronics Conf.*, May 1977, pp. 938-945.

[3] R.E. Ziemer and W.H. Tranter, *Principles of Communications; Systems, Modulation, and Noise.* Boston: Houghton-Mifflin, 1976, Appendix A.

[4] F.J. Harris, "On the use of windows for harmonic analysis with the discrete Fourier transform," *Proc. IEEE*, vol. 66, pp. 51-83, Jan. 1978.

0018-9251/80/0500-0397 $00.75 ©1980 IEEE